LA-UR 91-663

TITLE: DYNAMIC CORRELATIONS IN THE CLASSICAL TWO-DIMENSIONAL ANTIFERROMAGNETIC HEISENBERG MODEL WITH EASY-PLANE SYMMETRY

AUTHOR(S):
A. R. Volkel
G. M. Wysin*
A. R. Bishop
F. G. Mertens**

SUBMITTED TO: Physical Review B

Phys. Rev. B 44, 10,066 (1991).

*Dept. of Physics, Kansas State University
Manhattan, KS 66506

**Physics Institute, University of Bayreuth, D-8580
Bayreuth, Federal Republic of Germany

Los Alamos National Laboratory
Los Alamos, New Mexico 87545

FORM NO. 836 R4
ST. NO. 2629 5/81

Dynamic correlations in the classical two-dimensional antiferromagnetic Heisenberg model with easy-plane symmetry

A. R. Völkel, G. M. Wysin[+], A. R. Bishop, F. G. Mertens[*]
Theoretical Division and Center for Nonlinear Studies,
Los Alamos National Laboratory, Los Alamos, New Mexico 87545

We investigate the dynamics of the two-dimensional antiferromagnetic Heisenberg model with easy-plane exchange symmetry. We develop a phenomenology of spin wave and vortex excitations and calculate their contributions to the dynamical correlation functions $S^{\alpha\alpha}(\mathbf{q},\omega)$, $\alpha = x, y, z$. The vortex shape depends explicitly on an exchange anisotropy parameter λ and changes from a mainly in-plane structure below a critical λ_c to a shape with well established z components around the vortex center above λ_c. In this paper we will discuss only the case $\lambda < \lambda_c$ where the system behaves almost like the pure XY model. The general properties of the dynamical behavior of the spin waves and vortices below the Kosterlitz-Thouless transition temperature T_{KT} have been widely examined for the ferromagnetic XY model, and do not change much in the antiferromagnet (although here we have two magnon branches according to the two different spin sublattices). Our main interest is focused on the unbound vortices just above T_{KT}. Assuming a dilute gas of ballistically moving vortices, we obtain central peaks in $S^{\alpha\alpha}(\mathbf{q},\omega)$ similar to the ferromagnetic case, but in some cases at different positions in $\mathbf{q}$ space depending on whether the static vortex structure or the deviation from it due to a finite velocity dominates the correlations. These results are compared with a combined Monte Carlo-Molecular Dynamics simulation on a 100x100 square lattice. The phenomenological predictions for the correlation functions and the integrated intensities describe the numerical results quite well and, by comparing both methods we obtain values for the vortex correlation length, which are in good agreement with the Kosterlitz-Thouless theory.

PACS: 75.50.Ee, 75.10.Hk, 75.25.+z, 75.30.Ds

I Introduction

During the past few years an increasing interest in two-dimensional magnetic materials has developed. This is a result of (i) the investigation of a wide class of well-characterized quasi-two-dimensional magnetic materials which allow a detailed experimental study of their properties (inelastic neutron scattering, nuclear magnetic resonance, etc.), and (ii) the availability of high-speed computers with the capabilities for simulations on large lattices. Examples of these materials are : (1) layered magnets[6], like K_2CuF_4, Rb_2CrCl_4, $(CH_3NH_3)_2CuCl_4$, and $BaM_2(XO_4)_2$ with M = Co, Ni,... and X = As, P,...; (2) $CoCl_2$ graphite intercalation compounds[7]; (3) magnetic lipid layers[8], like $Mn(C_{18}H_{35}O_2)_2$ – here even monolayers can be produced, which are literally two-dimensional as concerns their magnetic properties.

Many of these materials have an "easy-plane" (XY) symmetry and the simplest classical model is described by the anisotropic Heisenberg Hamiltonian

$$H = J \sum_{<ij>} (S_i^x S_j^x + S_i^y S_j^y + \lambda S_i^z S_j^z). \tag{1.1}$$

Here $< i, j >$ label near-neighbor sites (which we take to be on a square lattice) and (x,y,z) spin components. $J < 0$ and $J > 0$ correspond to ferromagnetic and antiferromagnetic coupling, respectively, and $0 \leq \lambda < 1$ for XY spin symmetry.

The XY symmetry leads to a well-known topological phase transition[1] at a temperature T_{KT} (the "Kosterlitz-Thouless" transition). Below T_{KT}, vortex-antivortex spin configurations appear as thermal excitations in bound pairs, for $T > T_{KT}$, these bound states dissociate and the density of unbound vortices increases with T. At sufficiently high T, the mean spacing between unbound vortices approaches the vortex core size and diffusive spin dynamics results.

The static vortex spin configuration depends on the anisotropy parameter λ : for $\lambda < \lambda_c$ (≈ 0.72 on a square lattice[9]) static vortices are purely in-plane; for $\lambda > \lambda_c$ an additional out-of-plane component develops : the size of this S^z component increases with λ, allowing a continuous crossover to the isotropic Heisenberg limit ($\lambda = 1$), where the topological excitations are merons and instantons[10] rather than vortices.

The bound vortex pairs below T_{KT} only renormalize the shape of the spin wave peaks in the corelation functions while the free vortices above the phase transition should contribute to extra peaks. An earlier investigation of the dynamics of pairs of free vortices at $T = 0$ in ferromagnets (FM) and antiferromagnets

(AFM) showed that their motion crucially depends on their shape[11]. But so far a detailed study of the vortex dynamics above T_{KT} is available only for the FM with $\lambda < \lambda_c$[4,5], including in-plane symmetry breaking[12] and in-plane magnetic field[13]. There a phenomenology built on weakly interacting vortices moving ballistically between their interactions suggested central peaks (CP), with maximum weight at zero frequency in the dynamic spin correlation function, in good agreement with numerical simulations and experimental results for temperatures just above T_{KT}.

Most of the above mentioned materials, however, are AFMs – it is therefore obviously necessary to expand this vortex phenomenology to the AFM case. Here we have two different spin sublattices and for this reason also two spin wave branches which show up either purely in-plane or out-of-plane. The spatial vortex structure is almost the same as in the FM case leading to CP's with the same shape, but at different $\mathbf{q}$ values in the correlation functions. In the static vortex structure the spins are locally perfectly antiferromagnetically aligned, resulting in a CP around the Bragg point, while the deviations from this structure due to a finite vortex velocity point in the same direction for adjacent spins, leading to weak ferromagnetic behavior yielding small contributions to a peak at $\mathbf{q} = (0,0)$. For $\lambda < \lambda_c$ the static vortex structure is purely in-plane, leading to a squared Lorentzian CP at the Bragg point with an intensity that is decreasing with increasing vortex density. The only velocity dependent changes of this vortex structure are perpendicular to the easy plane and result in a Gaussian CP in the *out-of-plane* correlation function at $\mathbf{q} = (0,0)$ which is proportional to the number of vortices. Both in-plane and out-of-plane vortex CPs are in a $\mathbf{q}$ range where the corresponding spin wave branches also give a low frequency structure. But above T_{KT} the in-plane magnons almost disappear ("universal jump")[2] and the vortex CP is clearly visible. In the out-of-plane correlations, however, the spin waves are not affected by the phase transition and dominate over the vortex contributions for almost all q values.

A combined Monte Carlo-Molecular Dynamics (MC-MD) simulation on a 100x100 square lattice of the discrete system (1.1) using Landau-Lifshitz dynamics verifies our phenomenological results in a temperature regime $T_{KT} \lesssim T \lesssim 0.25 T_{KT}$ ($T_{KT} \approx 0.79 J S^2$); above this T range a diffusive spin motion becomes dominant. A fit of the in-plane correlation function to our theoretical result gives us values for the average vortex velocity and lower and upper bounds for the vortex correlation length.

The paper is organized as follows : in section (II) we discuss the different possible excitations in a system described by (1.1). In section (III) we calculate their contribution to the dynamical correlation function neglecting any interactions between them. The next section gives a short description of the MC-

MD simulation, and in section (V) we compare the numerical data with our phenomenological results. Section (VI) contains a brief summary.

II Excitations

1. Spin waves

The ground state of the classical two-dimensional antiferromagnetic isotropic Heisenberg model on a square lattice is the Neel state. Though this long-range order is destroyed at finite temperatures, Anderson[14] showed that the low lying excitations can be well described by a linear spin wave theory. The same is true for the anisotropic Heisenberg system where the spin wave spectrum was first calculated by Kanamori and Yosida[15] (with this easy-plane symmetry all the spins are confined to the XY plane for $T = 0$). Starting with the semi-classical Holstein-Primakoff ansatz[16] they obtained, after a few transformations (appendix A), the Hamiltonian in diagonalized form up to second order in this expansion : viz

$$H = -JS^2Nz + \sum_{\mathbf{q}} \{\hbar\omega_1(\mathbf{q})[\alpha_{\mathbf{q}}^+\alpha_{\mathbf{q}} + \tfrac{1}{2}] + \hbar\omega_2(\mathbf{q})[\beta_{\mathbf{q}}^+\beta_{\mathbf{q}} + \tfrac{1}{2}]\}, \tag{2.1}$$

where $\alpha_{\mathbf{q}}^+$, $\alpha_{\mathbf{q}}$, $\beta_{\mathbf{q}}^+$ and $\beta_{\mathbf{q}}$ are the creation and annihilation operators for the magnons, N is the total number of spins in the systems, and z is the number of nearest neighbors in the easy-plane. The frequencies are given by

$$\omega_1(\mathbf{q}) = 2JSz\sqrt{(1+\lambda\gamma(\mathbf{q}))\,(1-\gamma(\mathbf{q}))} \tag{2.2a}$$

and

$$\omega_2(\mathbf{q}) = 2JSz\sqrt{(1-\lambda\gamma(\mathbf{q}))\,(1+\gamma(\mathbf{q}))} \tag{2.2b}$$

with

$$\gamma(\mathbf{q}) = \frac{1}{z}\sum_{j=1}^{z} e^{i\rho_j\mathbf{q}}. \tag{2.3}$$

In this paper we will refer to ω_1 as the acustical and ω_2 as the optical spin wave branch. The ρ_j are the vectors to the nearest neighbors and on a square lattice ($z = 4$) with lattice constant $a = 1$ eqn. (2.3) reduces to

$$\gamma(\mathbf{q}) = \frac{1}{2}(\cos q_x + \cos q_y). \tag{2.4}$$

The two dispersion relations (2.2) are related to each other by the following symmetry

$$\omega_1(\mathbf{K}^0 - \mathbf{q}) = \omega_2(\mathbf{q}) \tag{2.5}$$

with $\mathbf{K}^0 = (\pi, \pi)$.

2. Vortices

The theory of Kosterlitz and Thouless[1] for phase transitions in two-dimensional systems with a continuously degenerate ground state suggests that, in addition to the spin waves, there will be topological excitations, namely vortices in this case. To obtain these vortices from the classical Hamiltonian (1.1) we have derived equations of motion[11] using an ansatz of Mikeska[17] containing four different angles

$$\begin{aligned} \mathbf{S}_i^{even} &= S\{\cos(\Phi_i + \phi_i)\sin(\Theta_i + \theta_i), \sin(\Phi_i + \phi_i)\sin(\Theta_i + \theta_i), \cos(\Theta_i + \theta_i)\}, \\ \mathbf{S}_j^{odd} &= -S\{\cos(\Phi_j - \phi_j)\sin(\Theta_j - \theta_j), \sin(\Phi_j - \phi_j)\sin(\Theta_j - \theta_j), \cos(\Theta_j - \theta_j)\}, \end{aligned} \tag{2.6}$$

where *even* and *odd* denote the two sublattices.

To find an analytical solution we work in the continuum limit. That is, we introduce two spin fields $\mathbf{S}^{even}(\mathbf{r})$ and $\mathbf{S}^{odd}(\mathbf{r})$ (or equivalently the fields $\Phi(\mathbf{r})$, $\Theta(\mathbf{r})$, $\phi(\mathbf{r})$, and $\theta(\mathbf{r})$) which are defined on the whole lattice and which are identical to (2.6) at the even or odd lattice sites, respectively. In this approximation it is easy to see (fig. 1) that the capital angles Φ and Θ describe the local antiferromagnetic alignment, while the small angles ϕ and θ describe deviations from it. These deviations point in the same direction for both the even and the odd sublattice – the dynamics expressed by these small angles will therefore show ferromagnetic behavior (see section III).

The four equations of motion for the angles introduced in (2.6) are fairly long and can be found in ref. 9. As in the ferromagnetic case[4,5] we find two different single vortex solutions which are stable for different regimes of λ. The two ranges are separated by a critical value λ_c which depends on temperature and on the density of vortices. (For a single static vortex on a 50x50 square lattice we find[9] $\lambda_c \approx 0.72$.) For $\lambda < \lambda_c$ the following "in-plane" vortex is stable, and has up to first order in the velocity v, the form

$$\begin{aligned} \Phi(\mathbf{r}) &= \tilde{q} \arctan\frac{y}{x} + \Phi_0 \\ \Theta(\mathbf{r}) &= \frac{\pi}{2} \\ \phi(\mathbf{r}) &= 0 \\ \theta(\mathbf{r}) &= f(r)\sin(\varphi - \epsilon). \end{aligned} \tag{2.7}$$

Here (r, φ) are cylindrical coordinates, $\tilde{q} = \pm 1, \pm 2, \ldots$ is the vorticity and ϵ is the angle between the direction of motion and the x-axis. For arbitrary λ the function $f(r)$ is given by

$$f(r) = \frac{\tilde{q}v}{JS} r \sum_{\nu=0}^{\infty} \frac{[4(1+\lambda)]^\nu r^{2\nu}}{\prod_{\mu=0}^{\nu}[\tilde{q}^2 - 4\lambda\mu(1+\mu)]} \tag{2.8}$$

with the asymptotic behavior

$$f(r) = \begin{cases} \frac{v}{\tilde{q}JS} r & r \to 0 \\ -\frac{\tilde{q}v}{4(1+\lambda)JS} \frac{1}{r} & r \to \infty \end{cases}, \tag{2.9}$$

while for $\lambda = 0$ we find the compact form

$$f(r) = \frac{\tilde{q}v}{JS} \frac{r}{\tilde{q}^2 - 4r^2}. \tag{2.10}$$

Eqn. (2.7) describes a vortex which is purely in-plane in the static case and which has some out-of-plane components proportional to the velocity which on one side of its direction of motion point above, and on the other side below, the plane.

For $\lambda > \lambda_c$ the following "out-of-plane" vortex is stable

$$\Phi(\mathbf{r}) = \tilde{q} \arctan \frac{y}{x}$$

$$\Theta(\mathbf{r}) = \begin{cases} \frac{c_3 r}{r_v} & r \to 0 \\ \frac{\pi}{2} - c_4 \sqrt{\frac{r_v}{r}} e^{-r/r_v} & r \to \infty \end{cases}$$

$$\phi(\mathbf{r}) = \cos(\varphi - \epsilon) \begin{cases} \frac{v}{JS} \frac{5+2\tilde{q}^2}{35+4\tilde{q}^2} r & r \to 0 \\ \frac{c_4 v}{JS} \frac{r_v}{8r_v^2+1} \sqrt{\frac{r_v}{r}} e^{-r/r_v} & r \to \infty \end{cases} \tag{2.11}$$

$$\theta(\mathbf{r}) = \sin(\varphi - \epsilon) \begin{cases} \frac{5c_3 v\tilde{q}}{JSr_v(35+4\tilde{q}^2)} r^2 & r \to 0 \\ -\frac{\tilde{q}v}{4(1+\lambda)JS} \frac{1}{r} & r \to \infty. \end{cases}$$

The constants c_3 and c_4 are determined by matching the asymptotic solutions of $\Theta(\mathbf{r})$ and

$$r_v = \frac{1}{2} \sqrt{\frac{\lambda}{1-\lambda}} \tag{2.12}$$

is the radius of the vortex core[5].

Both vortices have a static structure which is described only by the capital angles Φ and Θ and has the same form as in the ferromagnetic case except that we have here two sublattices with mutually antialigned spins. The deviations from these structures are small and are expressed by the angles ϕ and θ. These velocity dependent contributions are also almost identical to those of the ferromagnet; only in the large r limit do we obtain different results for the out-of-plane angle – in the denominator we have a factor $(1 - \lambda)$ in the ferromagnetic, but a factor $(1 + \lambda)$ in the antiferromagnetic model. θ describes

an out-of-plane structure where all the spins have a positive z component on one side of the direction of motion and a negative z component on the other side, even in the antiferromagnetic case (see (2.7) and (2.11)). Increasing λ means that the system becomes more isotropic and for the ferromagnet one needs less energy to orient the spins out of the plane. Conversely for the antiferromagnet, a similar consideration shows that the structure described by θ becomes less favourable for increasing λ. The factors $(1-\lambda)$ and $(1+\lambda)$ in the denominator of θ reflect this behavior for the two different models.

III Dynamical correlation functions

One of our goals in this paper is to calculate functions which reveal some of the dynamical properties of the system described by the Hamiltonian (1.1) and which are directly related to explicit measurements. A typical experiment to obtain such information from a magnetic system is inelastic neutron scattering where the results are proportional to the dynamical correlation functions $S^{\alpha\alpha}(\mathbf{q},\omega)$, $\alpha = x, y, z$, which we discuss in this section. We first start with some thoughts about how to deal with the two sublattices in an antiferromagnet. Then we will approximate the contributions from spin waves and free vortices to the in-plane and out-of-plane correlation functions. Due to the $O(2)$ symmetry in the easy-plane the functions S^{xx} and S^{yy} are equal to each other and we therefore will discuss only S^{xx} as the in-plane correlation function.

1. The magnetic structure factor for an antiferromagnet

In the antiferromagnet we have two sublattices with a different magnetic scattering behavior which can be expressed by the structure factor[17] $\Xi(\mathbf{K})$. For a short derivation of this structure factor we divide our system (fig. 2) in a square lattice (Bravais lattice) described by the vector

$$\mathbf{R} = 2(m\hat{a} + n\hat{b}), \quad m, n = 0, \pm 1, \pm 2, \ldots \tag{3.1}$$

with basis

$$\mathbf{r}_j \in \{0, \hat{a}, \hat{b}, \hat{a}+\hat{b}\} \tag{3.2}$$

(the lattice spacing is $a = 1$ and $\hat{a}$ and $\hat{b}$ are unit vectors). The reciprocal lattice vectors for (3.1) have the form

$$\mathbf{K} = \pi(\mu\hat{a} + \nu\hat{b}) \tag{3.3}$$

with μ, ν integers.

The magnetic structure factor is now simply the sum over the spin form factors e, which determine their scattering behavior, times a phase factor[18]

$$\Xi(\mathbf{Kr}) = \sum_{j=0}^{3} e_j e^{i\mathbf{K}\mathbf{r}_j}. \tag{3.4}$$

At $T = 0$ the antiferromagnet is in a perfect Neel state with spin form factors

$$e_0 = e_3 = +1 \quad \text{and} \quad e_1 = e_2 = -1. \tag{3.5}$$

Inserting (3.5) into (3.4) gives

$$\Xi = \begin{cases} 4 & \mu,\ \lambda \text{ odd integers} \\ 0 & \text{else.} \end{cases} \tag{3.6}$$

In this case a magnetic scattering experiment would only give a contribution at wave vectors

$$\mathbf{K}^0 = \pi(\sigma\hat{a} + \tau\hat{b}), \tag{3.7}$$

with $\sigma = 2\mu + 1$ and $\tau = 2\nu + 1$.

The spin form factors become more complicated for finite temperatures with spin waves and vortices present. However, the information in eqns. (3.6) and (3.7) allow us to define a sign function

$$e^{i\mathbf{K}^0\mathbf{r}} = \begin{cases} +1 & \mathbf{r} \text{ denoting an even lattice site} \\ -1 & \mathbf{r} \text{ denoting an odd lattice site,} \end{cases} \tag{3.8}$$

which helps us to take care of the different signs in the ansatz (2.6).

For the derivation of the correlation functions we will restrict ourselves to the first Brillouin zone and therefore only use the vector $\mathbf{K}^0 = (\pi, \pi)$. Furthermore we will introduce here the vector

$$\mathbf{q}^* = \mathbf{K}^0 - \mathbf{q}, \tag{3.9}$$

which gives us the q dependence of a function with respect to $\mathbf{K}^0$.

2. The contribution of spin waves to the correlation function

Because of the lack of long range order in our system for finite temperatures[19] there is no Bragg peak present in our system and the one-magnon processes should give the main contribution to the correlation function (at least for $T \lesssim T_{KT}$).

Using the results of appendix A, a straightforward calculation (appendix B) yields

$$\begin{aligned} S^{xx}(\mathbf{q},\omega) &= \frac{S}{2\pi}\int dt e^{-i\omega t} < \left[S^x(\mathbf{q},t)\right]^* S^x(\mathbf{q},0) > \\ &= \frac{S}{4\pi}\int dt e^{-i\omega t}\frac{\hbar\omega_2(\mathbf{q})}{2JSz(1+\gamma(\mathbf{q}))} < n_2(\mathbf{q})e^{-i\omega_2(\mathbf{q})t} + (n_2(\mathbf{q})+1)e^{i\omega_2(\mathbf{q})t} > \end{aligned} \tag{3.10}$$

and

$$\begin{aligned} S^{zz}(\mathbf{q},\omega) &= \frac{S}{2\pi}\int dt e^{-i\omega t} < \left[S^z(\mathbf{q},t)\right]^* S^z(\mathbf{q},0) > \\ &= \frac{S}{4\pi}\int dt e^{-i\omega t}\frac{\hbar\omega_1(\mathbf{q})}{2JSz(1+\lambda\gamma(\mathbf{q}))} < n_1(\mathbf{q})e^{-i\omega_1(\mathbf{q})t} + (n_1(\mathbf{q})+1)e^{i\omega_1(\mathbf{q})t} > . \end{aligned} \tag{3.11}$$

The in-plane (out-of-plane) correlation function depends only on $\omega_2(\mathbf{q})$ ($\omega_1(\mathbf{q})$), but this does not mean that ω_2 describes pure in-plane and ω_1 describes pure out-of-plane correlations. This can easily be seen by considering the spin waves in terms of the angles Φ, Θ, φ and θ as defined in (2.6). E.g. for the out-of-plane angles we find that Θ (which describes the local AFM ordering - cf. Sec. II.2) follows the ω_2-dispersion while θ (which describes the local FM ordering) follows the ω_1-dispersion. The (AFM) angle Θ, however, depends on $\mathbf{q}^*$, as was discussed in III.1 and therefore we have to consider the optical spin wave branche ω_2 with respect to the edge of the Brillouin zone. As a consequence of the symmetry (2.5) between the two spin wave branches we observe only one spin wave peak in S^{zz}. The same is true for S^{xx}.

The explicit line shape in eqns. (3.10) and (3.11) for the in-plane spin wave peak has the following asymptotic form[20]

$$S^{\alpha\alpha}(\mathbf{k},\omega) \propto \frac{1}{|\mathbf{k}|^{3-\eta_0}}\frac{1}{|1-w|^{1-\eta_0}} \tag{3.12a}$$

for $|w| \to 1$ and

$$S^{\alpha\alpha}(\mathbf{k},\omega) \propto \frac{1}{|\mathbf{k}|^{3-\eta_0}}\frac{1}{|w|^{3-\eta_0}} \tag{3.12b}$$

for $|w| \to \infty$ with the notation

$$w = \frac{\omega}{\omega_1(\mathbf{k})} \tag{3.13}$$

and

$$\mathbf{k} = \begin{cases} \mathbf{K}^0 - \mathbf{q} & \alpha = x \\ \mathbf{q} & \alpha = z. \end{cases} \tag{3.14}$$

The exponent

$$\eta_0 = \frac{k_B T}{4\pi J} \tag{3.15}$$

was first derived by Kosterlitz and Thouless[1] and has the value 1/4 at $T = T_{KT}$.

Below T_{KT} there also exist bound vortex-antivortex pairs which reduces the correlations between the spin waves. The effect of these additional excitations can be described by a renormalization[1,3] of (3.15), namely

$$\eta = \frac{\eta_0}{\epsilon(r \to \infty)}, \tag{3.16}$$

where $\epsilon(r)$ is a size dependent vortex dielectric function which makes the spin wave peak broader.

The divergence of the amplitude in (3.12a) is a feature of the infinitely extended system for which the whole derivation was made. Above T_{KT} the in-plane spin stiffness constant goes to zero discontinuosly ("universal jump") as was discussed by Nelson and Kosterlitz[2], and the spin wave theory in the easy-plane as presented here fails.

3. The contribution of free vortices to the correlation function

As mentioned in the previous section the bound vortex pairs below T_{KT} contribute only as a screening of the spin waves in the in-plane correlation function. Above T_{KT}, however, we expect that the unbound vortices give rise to an extra peak in $S^{\alpha\alpha}(\mathbf{q},\omega)$.

In our discussion we will restrict ourselves to temperatures just above T_{KT} where we assume that the vortices behave like a dilute gas of particles with average separation equal to by twice the correlation length ξ of the Kosterlitz-Thouless theory. Furthermore we consider only vortices with $|q| = 1$ which are the ones with lowest energy (the energy of a single vortex is proportional to the square of the vorticity[1]) and, to match with our simulations, we consider only the case $\lambda < \lambda_c$.

a) *In-plane correlation function*

The in-plane correlation function in the $(\mathbf{r},t)$ space is defined as

$$S^{xx}(\mathbf{r},t) = < [S^x(\mathbf{r},t)]^* S^x(0,0) > . \tag{3.17}$$

Inserting the solution (2.7) in (3.17) we obtain

$$S^{xx}(\mathbf{r},t) = S^2 < e^{i\mathbf{K}^0\mathbf{r}} \cos\Phi(\mathbf{r},t) \sin\left[\tfrac{\pi}{2} + e^{i\mathbf{K}^0\mathbf{r}}\theta(\mathbf{r},t)\right] \cos\Phi(0,0) \sin\left[\tfrac{\pi}{2} + \theta(0,0)\right] > . \tag{3.18}$$

S^{xx} is only globally sensitive to the presence of vortices – i. e. if we consider length scales much larger than the vortex core radius we can neglect the angle θ and the main effect of a vortex passing a lattice site is to change the sign of the spin at this place (i.e. to rotate the spin about 180°). In this approximation (3.18) reduces to

$$S^{xx}(\mathbf{r},t) = S^2 e^{i\mathbf{K}^0\mathbf{r}} < \cos^2\Phi > < (-1)^{N(\mathbf{r},t)} >, \tag{3.19}$$

where $N(\mathbf{r},t)$ is the number of vortices passing an arbitrary, nonintersecting contour between a spin at $(0,0)$ and the spin at $(\mathbf{r},t)$. Eqn. (3.19) has the same form as eqn. (2.4) in ref. 4. (The additional exponential factor will add to the exponentials of the Fourier transformation and yields only a different $\mathbf{q}$ dependence of $S^{zz}(\mathbf{q},\omega)$.) We can therefore follow exactly the calculation of Mertens et al.[4] to obtain, for the dynamical in-plane correlation function,

$$S^{zz}(\mathbf{q},\omega) = \frac{S^2}{2\pi}\frac{\gamma^3\xi^2}{\left\{\omega^2+\gamma^2[1+(\xi\mathbf{q}^*)^2]\right\}^2} \tag{3.20}$$

with

$$\gamma = \frac{\sqrt{\pi}\tilde{u}}{2\xi}, \tag{3.21}$$

and $\tilde{u}$ is the vortex average velocity. This is a squared Lorentzian central peak with its maximum in q space at $\mathbf{K}^0$.

A single vortex has the effect of disturbing the local Neel order in the vicinity of its core. For the in-plane correlation function this means that some of the intensity of the Bragg-peak is shifted to other q values. For a whole gas of single vortices (but with an average distance between the vortices much larger than the core radius, as assumed) we therefore expect to find a peak with its maximum at the Bragg-point and with a finite width in $\mathbf{q}$ and ω space. For the antiferromagnet this gives a peak at $\mathbf{q} = \mathbf{K}^0$ and $\omega = 0$ which is true for (3.20). Furthermore we see that the integrated intensity, see (5.1), is decreasing with the density of free vortices

$$n_v \propto (2\xi)^{-2}, \tag{3.22}$$

while the width is increasing, which we also expect from our previous discussion.

b) Out-of-plane correlation function

The out-of-plane correlation function is given by

$$S^{zz}(\mathbf{r},t) = < e^{i\mathbf{K}^0\mathbf{r}}\cos\left[\Theta(\mathbf{r},t)+e^{i\mathbf{K}^0\mathbf{r}}\theta(\mathbf{r},t)\right]\cos\left[\Theta(0,0)+\theta(0,0)\right] > . \tag{3.23}$$

Our vortex solutions are all given in the continuum limit which means that they are only valid beyond a certain distance from the vortex core (at least one lattice constant). Therefore we will use for our calculations only the large r limit of θ ($\Theta = \pi/2$) which should give a good approximation for small q values and reduces (3.23) to

$$S^{zz}(\mathbf{r},t) = < \theta(\mathbf{r},t)\theta(0,0) > . \tag{3.24}$$

Again we can follow the calculations of Mertens et al.[4] and also Gouvêa et al.[5] to obtain for the dynamical correlation function a Gaussian peak

$$S^{zz}(\mathbf{q},\omega) = \frac{n_v \tilde{u}}{32(1+\lambda)^2 J^2 \sqrt{\pi} q^3} e^{-\frac{\omega^2}{(\tilde{u}q)^2}}. \tag{3.25}$$

S^{zz} is sensitive to the explicit out-of-plane shape of the vortices and, because this structure has ferromagnetic order for $\lambda = 0$ (i.e. neighboring z components of both sublattices point in the same direction), we find a maximum at $\mathbf{q} = 0$ and $\omega = 0$ while the intensity of the peak is increasing with the density of free vortices n_v. Except for the plus sign in the factor $(1+\lambda)^2$ in the denominator, eqn. (3.25) is equivalent to the dynamical out-of-plane correlation function in the ferromagnetic model.

IV Simulations

For the numerical simulations we consider a 100x100 square lattice with periodic boundary conditions and $\lambda = 0$ (XY model). To obtain the dynamical correlation functions we basically follow three steps. (i) With a canonical ensemble MC algorithm we generate spin configurations for a given temperature. (ii) These data are used as input for a MD simulation realized by a fourth order Runge-Kutta method with time step $0.04/JS$ which integrates the Landau-Lifshitz equations of motion

$$\frac{d}{dt}\mathbf{S}_i = \mathbf{S}_i \times \mathbf{F}_i \tag{4.1}$$

with

$$\mathbf{F}_i = -\frac{\delta \mathrm{H}}{\delta \mathbf{S}_i} = -J \sum_{<i,j>} \left(S_j^x \hat{\mathbf{x}} + S_j^y \hat{\mathbf{y}} + \lambda S_j^z \hat{\mathbf{z}}\right) \tag{4.2}$$

($\hat{\mathbf{x}}, \hat{\mathbf{y}}, \hat{\mathbf{z}}$ are unit vectors parallel to the axis). Here, H is the Hamiltonian from eqn. (1.1) while the sum in (4.2) runs over all the nearest neighbors of the spin i. (iii) Finally a fast Fourier transformation gives us $S^{\alpha\alpha}(\mathbf{q},\omega)$, $\alpha = x, y, z$. To minimize the thermal and numerical fluctuations we used 10 initial configurations for the MD simulations, each separated by 2000 MC steps, for every temperature. These data are averaged before performing the time Fourier transformation.

A detailed description of the numerical simulations can be found in ref. 21.

V Discussion of the simulation results

For the following discussion we use dimensionless quantities, viz. we measure energies and temperatures in units of JS^2, frequencies in units of JS and lengths in units of the lattice constant a ($\hbar = k_B = 1$).

1. In-plane correlations

For the planar model Kosterlitz and Thouless[1] estimated a critical temperature for the vortex-pair unbinding of $T_{KT} \approx 0.89$. Due to our use of a $\lambda = 0$-anisotropic Heisenberg model[22] as well as finite size effects this temperature is smaller in our simulations and has a value of about $T_{KT} \approx 0.79$. Below this temperature $S^{zz}(\mathbf{q},\omega)$ displays a single peak with a dispersion displayed in fig. 3a and which we identify as the optical spin wave branch (2.2b) including a renormalization of the frequency due to thermal fluctuations, and with thermal broadening (increasing with T) caused by the scattering of spin waves.

This spin wave dispersion has its zero at $\mathbf{q} = \mathbf{K}^0$ where we also expect to find a central peak just above T_{KT} caused by unbound moving vortices. However, the softening of the spin stiffness constant in this temperature regime[2] allows us to observe this peak without a big overlap of magnon contributions (fig. 4) - for $\mathbf{q} = \mathbf{K}^0$ the spin waves disappear totally while for $\mathbf{q} \neq \mathbf{K}^0$ there are still some magnon contributions left in S^{zz}. Our phenomenology predicts a squared Lorentzian shape (3.20) for this peak. This result was derived in the large r limit treating the vortices as point-like excitations. Moreover, to make an analytical treatment possible Mertens et al.[4] replaced the exponent in $S^{zz}(\mathbf{r},t)$ by a convenient function which has almost the same shape as the original one. This substitution does not change the integrated intensity of $S^{zz}(\mathbf{q},\omega)$

$$I^z(\mathbf{q}) = \int_{-\infty}^{\infty} d\omega S^{zz}(\mathbf{q},\omega) = \frac{S^2}{4\pi} \frac{\xi^2}{[1+(q^*\xi)^2]^{\frac{1}{2}}}, \tag{5.1}$$

as can be checked directly by calculating

$$I^z(\mathbf{q}) = S^{zz}(\mathbf{q}, t=0) = (2\pi)^{-2} \int d^2\mathbf{q}\; S^{zz}(\mathbf{r}, t=0) \tag{5.2}$$

using the unchanged $S^{zz}(\mathbf{r},t)$ in (5.2). This q dependence of the intensity (5.1) is well supported by the MD data as can be seen in fig. 5 - the solid line in these pictures is a fit to the function given in (5.1) using only small values of q^* ($0 \leq q^* < 0.15\pi$) corresponding to the q range where the theory should be valid. The correlation lengths obtained by these fits are listed in table 1 and we will call these values ξ_1 for the remainder of this paper.

For our fits we used the total intensity of S^{zz} which for $\mathbf{q} \neq \mathbf{K}^0$ contains spin wave contributions in addition to the vortex ones. This overestimation results in a vortex correlation length which is systematically too short - therefore ξ_1 can be regarded as a lower bound of the real vortex correlation length of the system. Within the q range we used for our fits, S^{zz} exhibits only a single peak so that we are not

able to identify and substract the spin wave part. However, here the vortices strongly dominate over the spin wave contributions and the error in the correlation length should be small.

We also used the amplitude as a fitting parameter and the results are shown in table 2. Though we have neglected any internal structure of the vortices in our calculation the theoretical amplitudes $A_t = \xi_1^2/4\pi$ are only about a factor 3.3 larger than the values from the MD data. (The amplitude is given by $I^z(\mathbf{q} = \mathbf{K}^0)$ and therefore does not depend on the spin waves^2.)

So far we have discussed only a static quantity of the system, I^z, and found that it can be very well described by our phenomenology. However, we are mainly interested in whether the dynamics, as described by the correlation function, is also in agreement with our theory.

The q dependence of the *width* of the central peak is shown in fig. 6. The data are obtained by fitting S^{zz} with a squared Lorentzian of the form

$$L(\omega) = \frac{A}{\left[1 + (\sqrt{2} - 1)\left(\frac{\omega}{\Gamma}\right)^2\right]^2}, \tag{5.3}$$

where A is the amplitude, Γ is the width at half maximum, and both quantities are functions of the wavevector $\mathbf{q}$. These results are compared with the half width

$$\Gamma^z(q) = \frac{1}{2}\sqrt{\pi(\sqrt{2} - 1)}\ \frac{\tilde{u}}{\xi}\sqrt{1 + (\xi q^*)^2} \tag{5.4}$$

of the function (3.20) (solid line in fig. 6). For increasing q^* the remaining spin wave contributions in S^{zz} move away from $\omega = 0$ and we obtain values for the width from our fitting which are systematically larger than the one for the pure vortex peak (fig. 4b). Again, we use only data for small q^* ($0 \leq q^* < 0.15\pi$) where the vortex and the spin wave peaks lie on top of each other and we cannot distinguish between them. In this q regime the vortex intensity is much larger than the magnon intensity – that is why the estimate of the width obtained by fitting of S^{zz} to a single squared Lorentzian should already give us quite good values. The results should become even better for higher temperatures because of the renormalization of the spin wave frequencies to smaller ω with increasing T. These fits give us values for the correlation length (which we call here ξ_2), listed in table 1, and the average velocity, listed in table 3. Because of our overestimating of the width, we obtain values for the correlation length ξ_2 which are too large – thus ξ_2 has to be regarded as upper bound – and the true vortex correlation length ξ should therefore be within the range $\xi_1 \leq \xi \leq \xi_2$.

The temperature dependence of the correlation length is[1]

$$\xi(T) = \xi_0 e^{b/\sqrt{\tau}}, \tag{5.5}$$

where ξ_0 is of the order of unity, $\tau = (T - T_c)/T_c$ and b is a slightly T dependent number[23]. Neglecting this T dependence of b and averaging over the upper and lower bounds of ξ we obtain $b \approx 0.51$ for $T_c = 0.79$ (using only $T = 0.85,\ 0.90,\ 0.95\ ,1.00$). This value is much smaller than the result of Kosterlitz and Thouless[13] $(\pi/2)$ but is closer to results of a renormalization group analysis of Heinekamp and Pelcovitz[23].

The average velocity $\tilde{u}$ obtained by our fits also has to be regarded as upper bound, because it is determined by the linear slope of $\Gamma^s(\mathbf{q})$ for large q's (fig .6) and increases with an overestimation of the width. Especially for temperatures just above T_{KT}, only data for very small q values show an almost pure vortex behavior and the determination of $\tilde{u}$ becomes more uncertain.

As far as we are aware there exists only one theory for the dynamics of ballistically moving vortices[24] with a resulting mean velocity

$$\tilde{u} = \frac{\sqrt{\pi}}{2}\, e^{-b/\sqrt{\tau}} \left[b/\sqrt{\tau} + 0.58\right]^{\frac{1}{2}}. \tag{5.6}$$

This formula was developed for FM out-of-plane vortices and predicts an increase of $\tilde{u}$ for small τ and a nearly constant behavior above about $\tau = 4b^2 \approx 1.0$ (which corresponds to $T \approx 1.6$). Above $T = 0.85$ our fitted data show an increase of the average velocity with temperature (table 3) but the absolute values are about a factor 3 larger than we would expect from (5.6). On the other side, if we omit the value for $T = 1.05$ (where we already suspect diffusive behavior), our data seem to show a saturation of $\tilde{u}$ at about $T = 0.95$ which agrees with the data of the ferromagnet[4] at $\lambda = 0$.

However, (5.6) was developed using FM out-of-plane vortices which interact via an additional gyro-force between them and therefore show a quite a different dynamical behavior than the AFM (and also FM) in-plane vortices[11] which we have in our system ($\lambda = 0$). Therefore it is not clear whether our data should follow the predictions of Huber – a detailed study of the motion of in-plane vortices is in preparation (both theoretically and numerically).

A study of the dynamical correlations in an AFM with $\lambda = 0.8$, where the vortices have the out-of-plane structure (2.11), shows a temperature dependence of $\tilde{u}$ which is qualitatively consistent with the $\lambda = 0.0$ case (also for this case it is not clear, whether (5.6) should be valid, because we have no gyro force in AFM systems for all values of λ under consideration), but the absolute values for $\tilde{u}$ are

about twice as large as for $\lambda = 0.0$. From our investigation of the motion of pairs of free vortices at $T = 0$ we know, that out-of-plane vortices, in contrast to in-plane vortices, are not very sensitive to the discreteness (pinning) effects of the lattice because of their extended out-of-plane core structure. Though for $T \gtrsim T_{KT}$ the themal fluctuations are large enough to compensate the lattice pinning, we still expect that the mobility of the in-plane vortices is smaller as for the out-of-plane ones, giving rise to the different average velocities observed in our simulations. A detailed discussion of the AFM with $\lambda = 0.8$ will be presented elsewhere.

Above $T \approx 1.0$ the correlation length (and with it the average distance between two vortices) drops below two lattice constants and we expect that our model of ballistically moving vortices loses its validity while the motion of the spins becomes more diffusive. The change in the amplitude ratio A_t/A_{MD} of the integrated intensities from 3.3 to about 2 (table 2) seems to reflect this change in the dynamics, while a squared Lorentzian still is consistent with the shape of the central peak, leading us to the expectation that a theory of diffusive spin motion gives a shape which is similar to (3.20).

2. Out-of-plane correlations

We find, as expected from our discussions in section III.2, a single peak in $S^{zz}(\mathbf{q},\omega)$ for $T < T_{KT}$, which corresponds to the acoustical spin wave branch (fig. 3b) given by eqn. (2.2a). The spin stiffness constant of these out-of-plane magnons suffers no sudden softening at T_{KT} and we therefore can observe a clear spin wave peak even for high temperatures ($T = 1.05$).

The central peak caused by the freely moving vortices at $T \gtrsim T_{KT}$ as predicted by (3.25) is here centered at $\mathbf{q} = (0,0)$, which gives us again a strong overlap with the spin waves. The intensity of the vortex peak

$$I^z(\mathbf{q}) = \frac{n_v \bar{u}}{32\sqrt{\pi}} \frac{1}{q^2} \tag{5.8}$$

is proportional to the density of free vortices and therefore is expected to be small in the temperature range where our phenomenology should be valid. Fig. 7 shows MD data of the out-of-plane correlation function and the dashed line in these pictures is a plot of expression (3.25) with $\bar{u}$ and $n_v \approx (2\xi)^{-2}$ from the in-plane correlation function. The singularity in (5.8) for $q \to 0$ can be avoided by intrducing a cut-off function $\exp(-\epsilon r/\xi)$ with $\epsilon = O(1)$ (we use $\epsilon = 0.5$ for the curves in fig. 7) in order to account for the finite size of the vortices[5]. Thereby the eqn. (3.25) is changed by a factor $\chi^2(q)$ with

$$\chi(q) = \frac{\sqrt{\epsilon^2 + (q\xi)^2} - \epsilon}{\sqrt{\epsilon^2 + (q\xi)^2}}. \tag{5.9}$$

Close to $\mathbf{q} = (0,0)$ we observe a strong increase of the CP intensity in S^{zz} which is in good agreement with (3.25). Despite this increase of the vortex intensity with n_v we see from fig. 7 that S^{zz} is, even for high temperatures, clearly dominated by the spin waves for almost all q's so that we are not able to tell whether the CP has a Gaussian shape. However, the MD data for small $\mathbf{q}$ support our result for the CP width $\Gamma^z(\mathbf{q}) = \tilde{u}q = const$ for fixed q but varying temperatures (fig. 7a and c).

VI Conclusions

In the present paper we have investigated the dynamical behavior of the classical two-dimensional AFM Heisenberg model with easy-plane symmetry. First, we discussed the possible excitations – spin waves and vortices – and second, we examined their dynamics by studying the dynamical correlation functions $S^{\alpha\alpha}(\mathbf{q},\omega)$, $\alpha = x, y, z$.

There are two spin wave branches according to the two sublattices. One of them (the optical branch) is present only in the in-plane correlation function and shows above T_{KT} a sudden softening of the spin stiffness constant ("universal jump") as predicted in Ref. 2. The other (acoustical) shows purely in out-of-plane correlations and is not visibly affected by the KT phase transition.

There exist two different vortex solutions : below a critical λ_c the *in-plane* vortex (2.7) is stable while above T_{KT} the *out-of-plane* vortex (2.11) is stable. Both types of vortices have a static structure which has locally perfect AFM order while a finite velocity causes a deviation from this structure which points in the same direction for adjacent spins. In this paper we discussed only vortex dynamics for $\lambda < \lambda_c$.

Below T_{KT} the vortices are closely bound in pairs and their effect on S^{zz} can be described as a renormalization of the shape of the spin wave peak[1,3]. Above the critical temperature, however, the pairs begin to unbind, giving rise to additional central peaks (CP) in the correlation functions as in the FM case[4,5]. In contrast to the FM , where we find the CP's centered at $\mathbf{q} = (0,0)$ for both in-plane and out-of-plane correlations, we have a different scenario in the AFM : the static structure contributes to a CP centered at $\mathbf{q} = \mathbf{K}^0$ while the additional structure due to motion gives a CP centered at $\mathbf{q} = (0,0)$, and especially for $\lambda < \lambda_c$, we have a CP at $\mathbf{q} = \mathbf{K}^0$ in S^{xx} and one at $\mathbf{q} = (0,0)$ in S^{zz}.

The in-plane CP in our simulation data (for $\lambda = 0$) can be well-explained by the squared Lorentzian shape (3.20) and the $\mathbf{q}$ dependence of the widths and intensities of these peaks are in good agreement with our phenomenolgical result up to a temperature $T \approx 1.0$ – our vortex phenomenology therefore seems to be a good approximation for a temperature range of about $T_{KT} \lesssim T \lesssim 1.25 T_{KT}$. Through fitting

the MD data with our theory we obtain values for the vortex length, which are in good agreement with the KT theory[1], and the vortex rms average velocity $\bar{u}$. A comparison of $\bar{u}$ with the formula of Huber[24] developed for FM out-of-plane vortices shows a reasonable agreement, but an extension of these results of Huber to the in-plane case may be appropriate : this is in preparation.

In the out-of-plane correlation function an analysis of the vortex CP is difficult, because it is dominated by the spin wave peak for almost all q values. We can therefore not unequivocally decide whether it has the Gaussian shape (3.25), but the MD data for small q values show a CP with constant width, consistent with our predictions.

For $\lambda > \lambda_c$ with or without an applied magnetic field we expect to have even more vortex peaks for the AFM (at $\mathbf{q} = (0,0)$ and $\mathbf{q} = \mathbf{K}^0$ for both, S^{xx} and S^{zz}). Each of these peaks is dominated by one of the four angles introduced in (2.6) and we therefore can investigate the different (static, dynamic, field induced) contributions from vortices to the dynamical correlation function seperately. Detailed analysis of these cases will be presented elsewhere.

Acknowledgements

This work was supported by the NATO (Collaborative Research Grant 0013/89) and by the United States Department of Energy and by Deutsche Forschungsgemeinschaft (project C19, SFB 213).

Appendix A

Without any loss of generality we assume here that for $T = 0$ all spins are parallel to the y-axis. With a Holstein-Primakoff ansatz[16] up to second order in the Boson operators we obtain

$$\begin{aligned} S_i^+ &= S_i^z + iS_i^x \cong \sqrt{2S}a_i \\ S_i^- &= S_i^z - iS_i^x \cong \sqrt{2S}a_i^* \\ S_i^y &= S - a_i^* a_i \end{aligned} \tag{A.1}$$

$$\begin{aligned} S_j^+ &= S_j^z + iS_j^x \cong \sqrt{2S}b_i^* \\ S_j^- &= S_j^z - iS_j^x \cong \sqrt{2S}b_i \\ S_j^y &= -S + b_j^* b_j . \end{aligned} \tag{A.2}$$

We now transform to the Fourier space with

$$\begin{aligned} a_{\mathbf{q}} &= \sqrt{\frac{2}{N}} \sum_i a_i e^{-i\mathbf{q}\mathbf{r}_i} \\ b_{\mathbf{q}} &= \sqrt{\frac{2}{N}} \sum_j b_j e^{i\mathbf{q}\mathbf{r}_j} . \end{aligned} \tag{A.3}$$

Restricting ouerselves to half of the Brillouin zone we eliminate of all the terms with mixed plus and minus $\mathbf{q}$ terms by the transformation

$$\begin{aligned} A_{\mathbf{q}_1} &= \frac{1}{\sqrt{2}}(a_{\mathbf{q}} + a_{-\mathbf{q}}); \quad A_{\mathbf{q}_2} = \frac{1}{\sqrt{2}}(a_{\mathbf{q}} - a_{-\mathbf{q}}) \\ B_{\mathbf{q}_1} &= \frac{1}{\sqrt{2}}(b_{\mathbf{q}} + b_{-\mathbf{q}}); \quad B_{\mathbf{q}_2} = \frac{1}{\sqrt{2}}(b_{\mathbf{q}} - b_{-\mathbf{q}}). \end{aligned} \tag{A.4}$$

Here $A_{\mathbf{q}_1}$ ($B_{\mathbf{q}_1}$) and $A_{\mathbf{q}_2}$ ($B_{\mathbf{q}_2}$) are operating on different subsets of the $\mathbf{q}$ space, but together they cover the whole Brillouin zone. Now we transform to real operators according to

$$\begin{aligned} Q_{\mathbf{q}_l} &= \frac{1}{\sqrt{2}}(A_{\mathbf{q}_l} + A^*_{\mathbf{q}_l}); \quad P_{\mathbf{q}_l} = \frac{1}{i\sqrt{2}}(A_{\mathbf{q}_l} - A^*_{\mathbf{q}_l}) \\ R_{\mathbf{q}_l} &= \frac{1}{\sqrt{2}}(B_{\mathbf{q}_l} + B^*_{\mathbf{q}_l}); \quad S_{\mathbf{q}_l} = \frac{1}{i\sqrt{2}}(B_{\mathbf{q}_l} - B^*_{\mathbf{q}_l}) \end{aligned} \tag{A.5}$$

with $l = 1, 2$. Finally after the transformation

$$\begin{aligned} q_{\mathbf{q}_l} &= \frac{1}{\sqrt{2}}(Q_{\mathbf{q}_l} + R_{\mathbf{q}_l}); \quad p_{\mathbf{q}_l} = \frac{1}{\sqrt{2}}(Q_{\mathbf{q}_l} - R_{\mathbf{q}_l}) \\ r_{\mathbf{q}_l} &= \frac{1}{\sqrt{2}}(P_{\mathbf{q}_l} + S_{\mathbf{q}_l}); \quad s_{\mathbf{q}_l} = \frac{1}{\sqrt{2}}(P_{\mathbf{q}_l} - S_{\mathbf{q}_l}), \end{aligned} \tag{A.6}$$

where $(p_{\mathbf{q}_l}, q_{\mathbf{q}_l})$ and $(s_{\mathbf{q}_l}, r_{\mathbf{q}_l})$ are pairs of canonically conjugate variables, we obtain the Hamiltonian in the form of harmonic oscillators

$$\begin{aligned} H = E_0 + JSz \sum_{\mathbf{q}_1} \{ &(1 - \gamma(\mathbf{q}))p^2_{\mathbf{q}_1} + (1 + \lambda\gamma(\mathbf{q}))q^2_{\mathbf{q}_1} \\ &+ (1 + \gamma(\mathbf{q}))s^2_{\mathbf{q}_1} + (1 - \lambda\gamma(\mathbf{q}))r^2_{\mathbf{q}_1} \} \\ + JSz \sum_{\mathbf{q}_2} \{ &(1 - \lambda\gamma(\mathbf{q}))p^2_{\mathbf{q}_2} + (1 + \gamma(\mathbf{q}))q^2_{\mathbf{q}_2} \\ &+ (1 + \lambda\gamma(\mathbf{q}))s^2_{\mathbf{q}_2} + (1 - \gamma(\mathbf{q}))r^2_{\mathbf{q}_2} \}. \end{aligned} \tag{A.7}$$

From (A.7) we obtain two dispersion curves

$$\begin{aligned} \omega_1(\mathbf{q}) &= 2JSz\sqrt{(1 + \lambda\gamma(\mathbf{q}))(1 - \gamma(\mathbf{q}))} \\ \omega_2(\mathbf{q}) &= 2JSz\sqrt{(1 - \lambda\gamma(\mathbf{q}))(1 + \gamma(\mathbf{q}))} \end{aligned} \tag{A.8}$$

with

$$\gamma(\mathbf{q}) = \frac{1}{z}\sum_{m=1}^{z} e^{i\rho_m \mathbf{r}_l}. \tag{A.9}$$

[$p_{\mathbf{q}_1}, s_{\mathbf{q}_2}$ are the momentum and $q_{\mathbf{q}_1}, r_{\mathbf{q}_2}$ are the position operators for the acoustic magnon branch ($\omega_1(\mathbf{q})$) for all $\mathbf{q}$ values, and analogous $p_{\mathbf{q}_2}, s_{\mathbf{q}_1}$ and $q_{\mathbf{q}_2}, r_{\mathbf{q}_1}$ for the optic magnon branch ($\omega_2(\mathbf{q})$)].

Finally we can express the operators in (A.7) through creation and annihilation operators α for the acoustic and β for the optic branch to obtain the Hamiltonian in its diagonalized form

$$H = E_0 + \sum_{\mathbf{q}} \left\{ \hbar\omega_1(\mathbf{q})(\alpha^+_{\mathbf{q}}\alpha_{\mathbf{q}} + \tfrac{1}{2}) + \hbar\omega_2(\mathbf{q})(\beta^+_{\mathbf{q}}\beta_{\mathbf{q}} + \tfrac{1}{2}) \right\}. \tag{A.10}$$

Appendix B

a) *In-plane correlation function*

If we define the Boson operators a_i (b_j) also on the odd (even) sublattice then we can write the x components of the spins as

$$\begin{aligned} S^x_i &= -i\frac{\sqrt{S}}{2\sqrt{2}}\left\{(a_i - a^*_i + b^*_i - b_i) + (a_i - a^*_i - b^*_i + b_i)\right\} \\ S^x_j &= -i\frac{\sqrt{S}}{2\sqrt{2}}\left\{(a_j - a^*_j + b^*_j - b_j) - (a_j - a^*_j - b^*_j + b_j)\right\}. \end{aligned} \tag{B.1}$$

Using the "sign function" (3.8) we can rewrite (B.1) in a single line

$$S^x_h = -i\frac{\sqrt{S}}{2\sqrt{2}}\left\{(a_h - a^*_h + b^*_h - b_h) + e^{i\mathbf{K}^0\mathbf{r}_h}(a_h - a^*_h - b^*_h + b_h)\right\} \tag{B.2}$$

with h running over all the lattice sites.

The dynamic in-plane correlation function is defined by

$$\begin{aligned} S^{xx}(\mathbf{q},\omega) &= \frac{1}{2\pi}\int dt e^{-i\omega t}\frac{1}{N^2}\sum_{m,n} < \left[S^x(\mathbf{r}_m,t)\right]^* S^x(\mathbf{r}_n,0) > \\ &= \frac{1}{2\pi}\int dt e^{-i\omega t} < \left[S^x(\mathbf{q},t)\right]^* S^x(\mathbf{q},0) > . \end{aligned} \tag{B.3}$$

Using (B.1) and without explicitly considering the time dependence we obtain

$$S^x(\mathbf{q}) = -i\frac{\sqrt{S}}{2\sqrt{2}}\left\{a_{\mathbf{q}} - a^*_{-\mathbf{q}} + b^*_{\mathbf{q}} - b_{-\mathbf{q}} + a_{-\mathbf{q}^*} - a^*_{\mathbf{q}^*} - b^*_{-\mathbf{q}^*} + b_{\mathbf{q}^*}\right\} \tag{B.4}$$

or, in terms of the creation and annihilation operators of the magnons,

$$S^x(\mathbf{q}) = -i\frac{\sqrt{S}}{2\sqrt{2}}\sqrt{\frac{\hbar\omega_2(\mathbf{q})}{2JSz(1+\gamma(\mathbf{q}))}}\left\{\beta_{\mathbf{q}_1} - \beta^+{}_{\mathbf{q}_1} + \beta^+{}_{\mathbf{q}_2} + \beta_{\mathbf{q}_2} + \alpha_{\mathbf{q}_1^*} - \alpha^+{}_{\mathbf{q}_1^*} - \alpha^+{}_{\mathbf{q}_2^*} + \alpha_{\mathbf{q}_2^*}\right\}. \tag{B.5}$$

In (B.5) we made use of the symmetry property of the frequencies (2.5). After inserting (B.5) in (B.3) and after a straightforward calculation we obtain

$$S^{xx}(\mathbf{q},\omega) = \frac{S}{8\pi}\int dt e^{-i\omega t}\frac{\hbar\omega_2(\mathbf{q})}{2JSz(1+\gamma(\mathbf{q}))}\cdot$$

$$< n_2(\mathbf{q})e^{-i\omega_2(\mathbf{q})t} + (n_2(\mathbf{q})+1)e^{i\omega_2(\mathbf{q})t} + n_1(\mathbf{q}^*)e^{-i\omega_1(\mathbf{q}^*)t} + (n_1(\mathbf{q}^*)+1)e^{i\omega_1(\mathbf{q}^*)t} > \qquad (B.6)$$

with

$$n_l(\mathbf{q}) = \alpha^+_{\mathbf{q}_l}\alpha_{\mathbf{q}_l} + \alpha^+_{\mathbf{q}_l^*}\alpha_{\mathbf{q}_l^*}, \quad l = 1,2. \qquad (B.7)$$

Using eqn. (2.5) we can write down a similar equation for the number of excited magnons, viz

$$n_1(\mathbf{q}^*) = n_2(\mathbf{q}). \qquad (B.8)$$

Therefore we finally obtain for the dynamic in-plane correlation function

$$S^{xx}(\mathbf{q},\omega) = \frac{S}{4\pi}\int dt e^{-i\omega t}\frac{\hbar\omega_2(\mathbf{q})}{2JSz(1+\gamma(\mathbf{q}))} < n_2(\mathbf{q})e^{-i\omega_2(\mathbf{q})t} + (n_2(\mathbf{q})+1)e^{i\omega_2(\mathbf{q})t} > . \qquad (B.9)$$

b) Out-of-plane correlation function

For the z components an ansatz of the spins as in (B.2) yields

$$S^z_h = \frac{\sqrt{S}}{2\sqrt{2}}\{(a_h + a^*_h + b^*_h + b_h) + e^{i\mathbf{K}^0\mathbf{r}_h}(a_h + a^*_h - b^*_h - b_h)\} \qquad (B.10)$$

or, similarly to (B.5),

$$S^z(\mathbf{q}) = \frac{\sqrt{S}}{2\sqrt{2}}\sqrt{\frac{\hbar\omega_1(\mathbf{q})}{2JSz(1+\lambda\gamma(\mathbf{q}))}}\{\alpha_{\mathbf{q}_1} + \alpha^+{}_{\mathbf{q}_1} - \alpha^+{}_{\mathbf{q}_2} + \alpha_{\mathbf{q}_2} + \beta_{\mathbf{q}_1^*} + \beta^+{}_{\mathbf{q}_1^*} + \beta^+{}_{\mathbf{q}_2^*} - \beta_{\mathbf{q}_2^*}\}. \qquad (B.11)$$

Thus the spin wave contribution to the dynamic out-of-plane correlation function becomes

$$S^{zz}(\mathbf{q},\omega) = \frac{S}{4\pi}\int dt e^{-i\omega t}\frac{\hbar\omega_1(\mathbf{q})}{2JSz(1+\lambda\gamma(\mathbf{q}))} < n_1(\mathbf{q})e^{-i\omega_1(\mathbf{q})t} + (n_1(\mathbf{q})+1)e^{i\omega_1(\mathbf{q})t} > . \qquad (B.12)$$

+ Permanent address : Departement of Physics, Kansas State University, Manhattan, Kansas 66506, USA.

* Permanent address : Physics Institute, University of Bayreuth, D-8580 Bayreuth, Federal Republic of Germany.

1. J. M. Kosterlitz, D. J. Thouless, *J. Phys.* **C6** 1181 (1973)

2. D. R. Nelson, J. M. Kosterlitz, *Phys. Rev. Lett.* **39** 1201 (1977)

3. R. Côté, A. Griffin, *Phys. Rev.* **B34** 6240 (1986)

4. F. G. Mertens, A. R. Bishop, G. M. Wysin, C. Kawabata, *Phys. Rev.* **B39** 591 (1989)

5. M. E. Gouvêa, G. M. Wysin, A. R. Bishop, F. G. Mertens, *Phys. Rev.* **B39** 11840 (1989)

6. K. Hirakawa, H. Yoshizawa, K. Ubukoshi, *J. Phys. Soc. Jpn.* **51** 2151 (1982)
   S. T. Bramwell, M. T. Hutchings, J. Norman, R. Pynn, P. Day, *J. Physique* **C8** 1435 (1988)
   M. Aïn, *J. Physique* **48** 2103 (1987)
   L. P. Regnault, J. P. Boucher, J. Rossat-Mignot, J. Bouillot, R. Pynn, J. Y. Henry, J. P. Renard, *Physica B+C* **136B** 329 (1986)
   L. P. Regnault, C. Lartigue, J. F. Legrand, B. Farago, J. Rossat-Mignod, J. Y. Henry, International Conference on Neutron Scattering, Grenoble (1988)

7. D. G. Wiesler, H. Zabel, S. M. Shapiro, International Conference on Neutron Scattering, Grenoble (1988)

8. M. Pomerantz, *Surface Science* **142** 556 (1984)
   D. I. Head, B. H. Blott, D. Melville *J. Physique* **C8** 1649 (1988)

9. G. M. Wysin, in *Computational Physics and Cellular Automata*, eds. A. Pires, D. P. Landau,H. Herrmann, World Scientific, p.29 (1990)

10. A. A. Belavin, A. M. Polyakov, Pis'ma Zh. Eksp. Teor. Fiz. **22** 503 (1975) [*JETP Lett.* **22** 245 (1975)]

11. A. R. Völkel, F. G. Mertens, A. R. Bishop, G. M. Wysin, *to be published in Phys. Rev. B*

12. M. E. Gouvêa, G. M. Wysin, A. R. Bishop, F. G. Mertens, *J. Phys.: Condens. Matter* **1** 4387 (1989)

13. M. E. Gouvêa, F. G. Mertens, A. R. Bishop, G. M. Wysin, *J. Phys.: Condens. Matter* **2** 1853 (1990)

14. P. W. Anderson, *Phys. Rev.* **86** 694 (1952)

15. J. Kanamori, K. Yosida, *Prog. Theor. Phys.* **14** 423 (1955)

16. T. Holstein, H. Primakoff, *Phys. Rev.* **58** 1098 (1940)

17. H. J. Mikeska, *J. Phys.* **C13** 2913 (1980)

18. C. Kittel *Introduction to Solid State Physics*, John Wiley & Sons, Inc., New York (1986)

19. N. D. Mermin, H. Wagner, *Phys. Rev. Lett.* **28** 1133 (1966)
    P. C. Hohenberg, *Phys. Rev.* **158** 383 (1967)

20. H. J. Mikeska, *Solid State Comm.* **13** 73 (1973)
    D. R. Nelson, D. S. Fisher, *Phys. Rev.* **B16** 4945 (1977)

21. G. M. Wysin, A. R. Bishop, *Phys. Rev.* **B42** 810 (1990)

22. Kawabata, *Solid State Comm.* 60 169 (1986)

23. S. W. Heinekamp, R. A. Pelcovitz, *Phys. Rev.* **B32** 4528 (1985)

24. D. L. Huber, *Phys. Rev.* **B26** 3758 (1982)

table 1 *Vortex correlation lengths above T_{KT} (units as defined at the beginning of chapter V);*

ξ_1 : *values obtained by fitting the integrated intensity with (5.1);*

ξ_2 : *values obtained by fitting the width of S^{zz} with (5.4).*

T	ξ_1	ξ_2
0.85	4.60	9.08
0.90	3.69	5.28
0.95	2.43	4.35
1.00	2.09	3.28
1.05	1.54	3.17

****

table 2 *Amplitudes of the integrated intensity $I^z(\mathbf{q} = \mathbf{K}^0)$;*

A_{MD} : *data from MD simulations;*

A_t : *theoretical amplitude (cf text).*

T	A_{MD}	A_t	A_t/A_{MD}
0.85	0.61	1.79	2.93
0.90	0.35	1.32	3.77
0.95	0.18	0.58	3.22
1.00	0.13	0.42	3.23
1.05	0.09	0.19	2.11

table 3 *Vortex average velocities;*

$\bar{u}$: *values obtained by fitting the width of* S^{zz} *with (5.4);*

$\bar{u}_H$: *values obtained by using the formula of Huber (5.6).*

T	$\bar{u}$	$\bar{u}_H$
0.85	1.17	0.22
0.90	0.96	0.32
0.95	1.05	0.37
1.00	1.05	0.41
1.05	1.13	0.44

Fig. 1 Definition of the in-plane angles Φ and ϕ (cf text).

Fig. 2 a) Square lattice defined by $\mathbf{R}$ (3.1) with b) basis $\mathbf{r}_i$ (3.2); • and ○ denote spins of the even and odd sublattice, respectively.

Fig. 3 Spin wave dispersion along the (q,q)-direction for a) the in-plane (optical) and b) the out-of-plane (acoustical) magnon branch; solid line : $T = 0$ (theoretical result (2.2)); + : $T = 0.3$; ◇ : $T = 0.5$.

Fig. 4 In-plane correlation function S^{xx} for different temperatures and wave vectors: solid line : MD data; dashed line : fit to squared Lorentzian (5.3).

Fig. 5 In-plane integrated intensity $I^x(\mathbf{q})$ for a) $T = 0.9$ and b) $T = 1.0$; + : intensity of fitted squared Lorentzian; ◇ : intensity from MD simulation; solid line : fit for small q^* to (5.1).

Fig. 6 Width $\Gamma^x(\mathbf{q})$ of the in-plane correlation function for a) $T = 0.9$ and b) $T = 1.0$; + : data from fitting S^{xx} with (5.3); solid line : fit for small q^* to (5.4).

Fig. 7 Out-of-plane correlation finction S^{zz} for different temperatures and wave vectors; solid line : MD data; dashed line : estimated vortex contribution using (3.25)$*\chi^2(q)$ (cf chapter V.2).

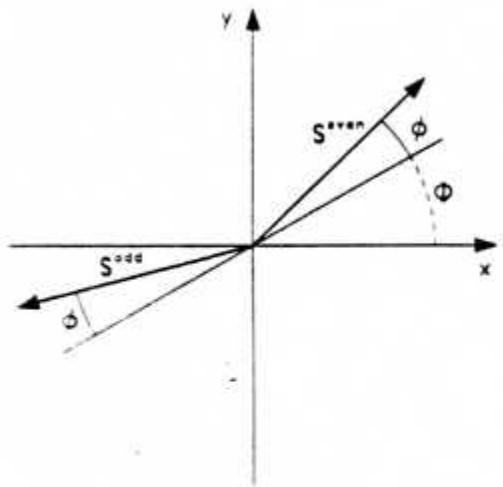

Fig 1

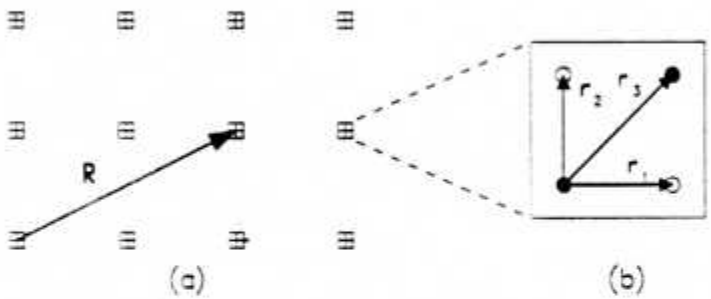

fig 2

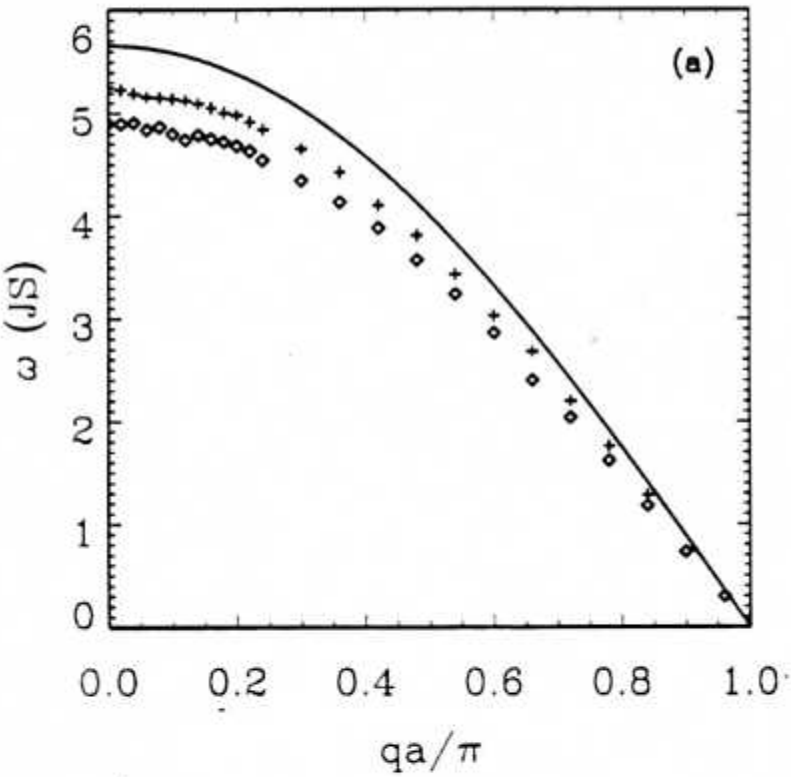

fig 3a

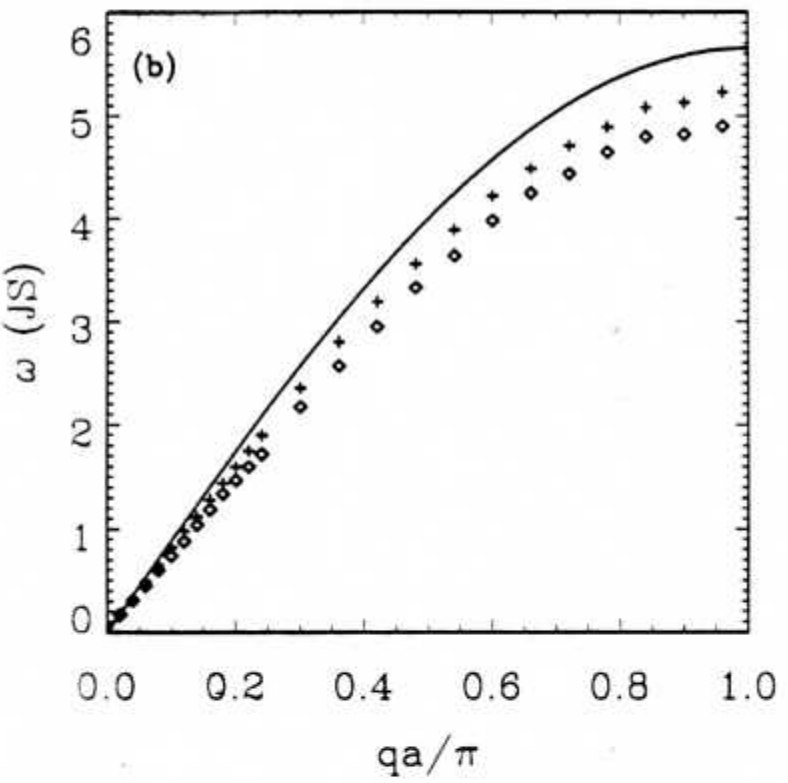

fig 3b

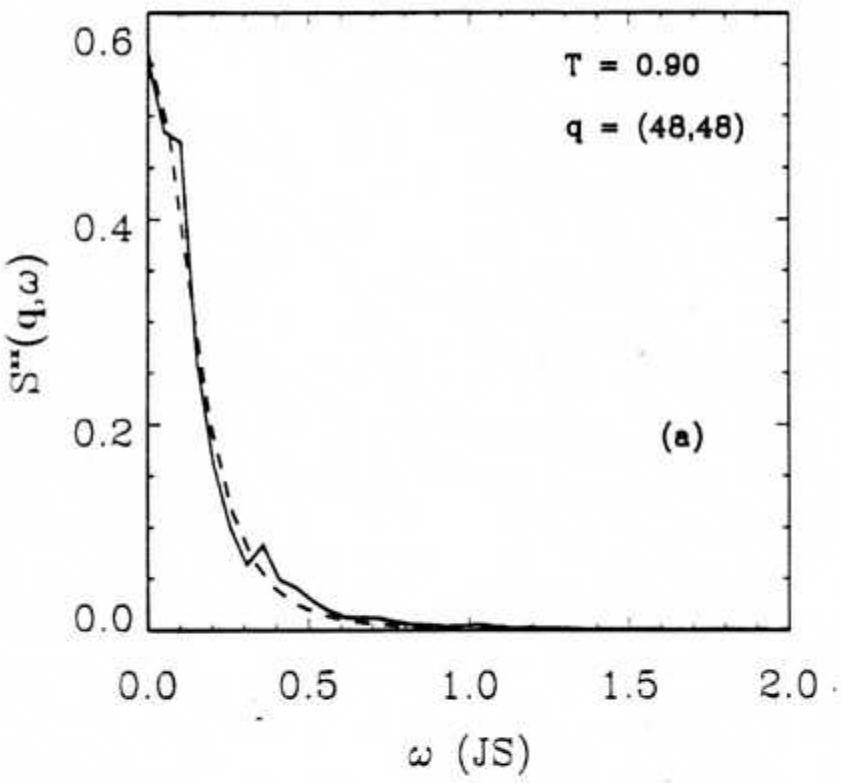

fig 4a

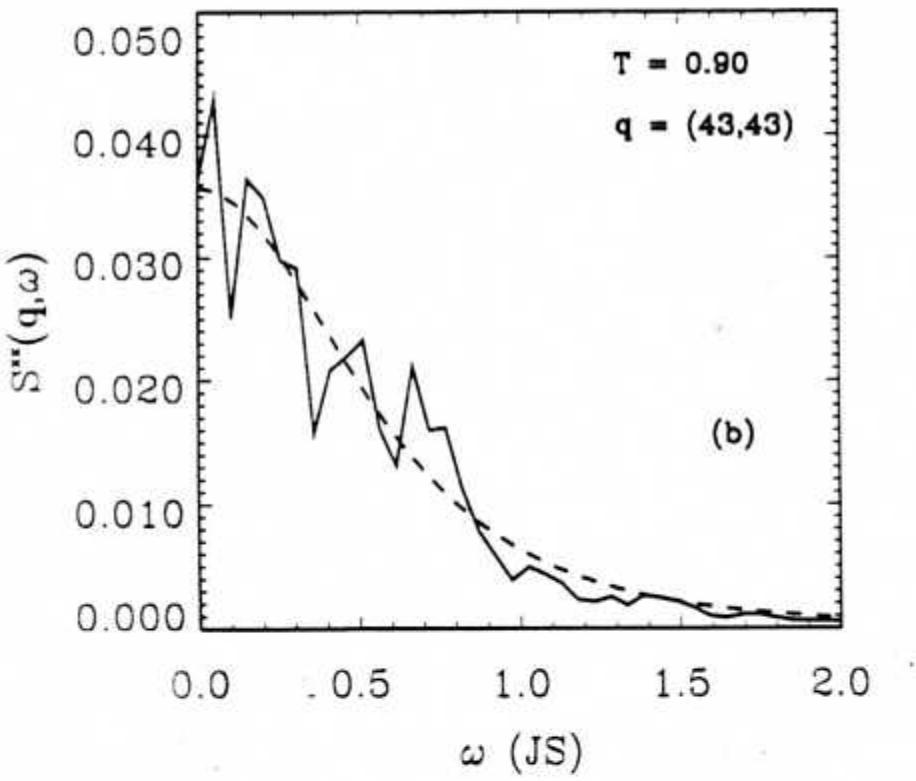
T = 0.90
q = (43,43)
(b)
0.050
0.040
0.030
0.020
0.010
0.000
0.0
0.5
1.0
1.5
2.0
ω (JS)
S''(q,ω)

fig 4b

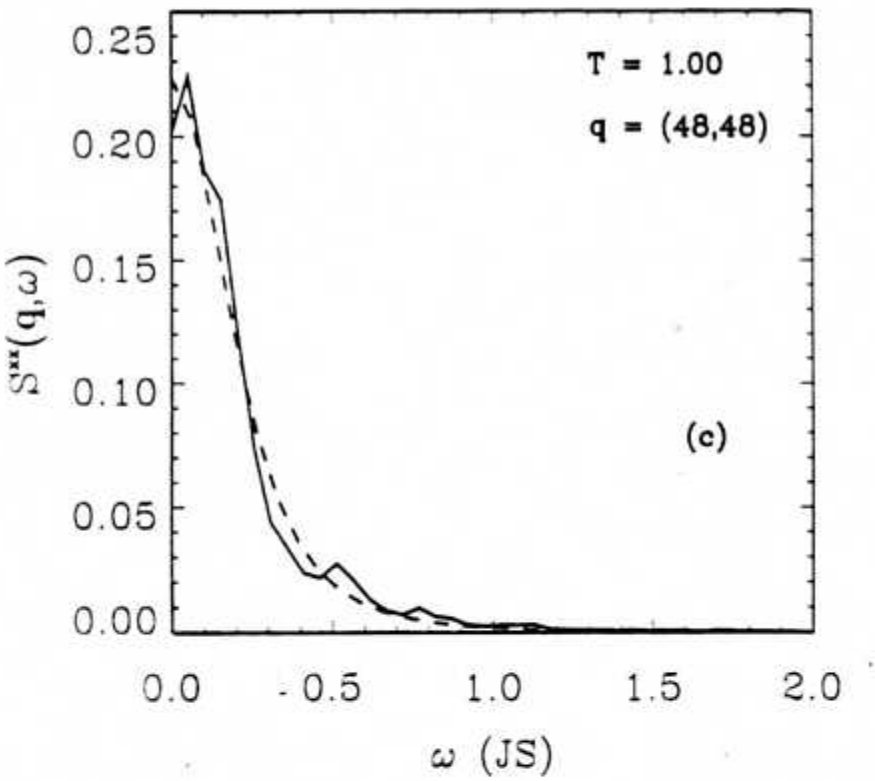
0.25
0.20
0.15
0.10
0.05
0.00
$S^{xx}(q,\omega)$
T = 1.00
q = (48,48)
(c)
0.0
- 0.5
1.0
1.5
2.0
ω (JS)

fig 4c

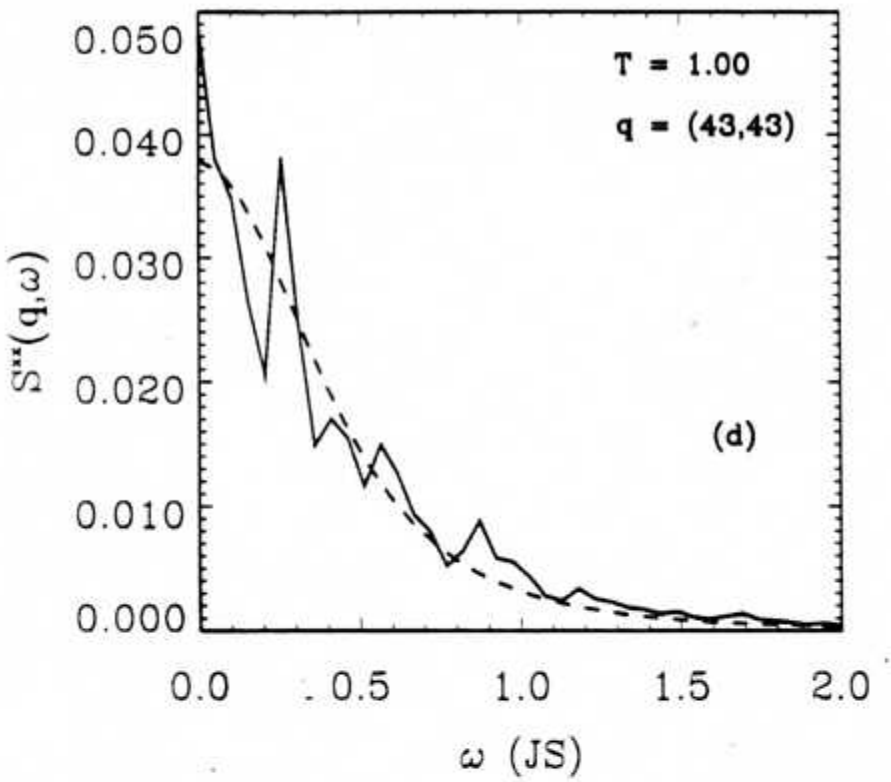
0.050
0.040
0.030
0.020
0.010
0.000
$S^{zz}(q,\omega)$
T = 1.00
q = (43,43)
(d)
0.0
0.5
1.0
1.5
2.0
ω (JS)

Fig-4d

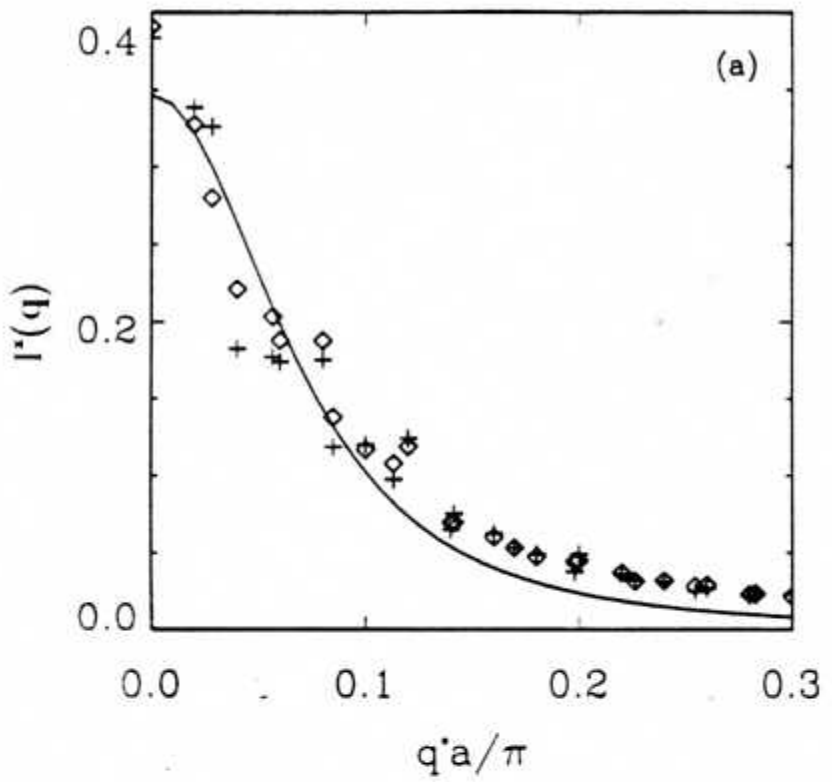

fig 5a

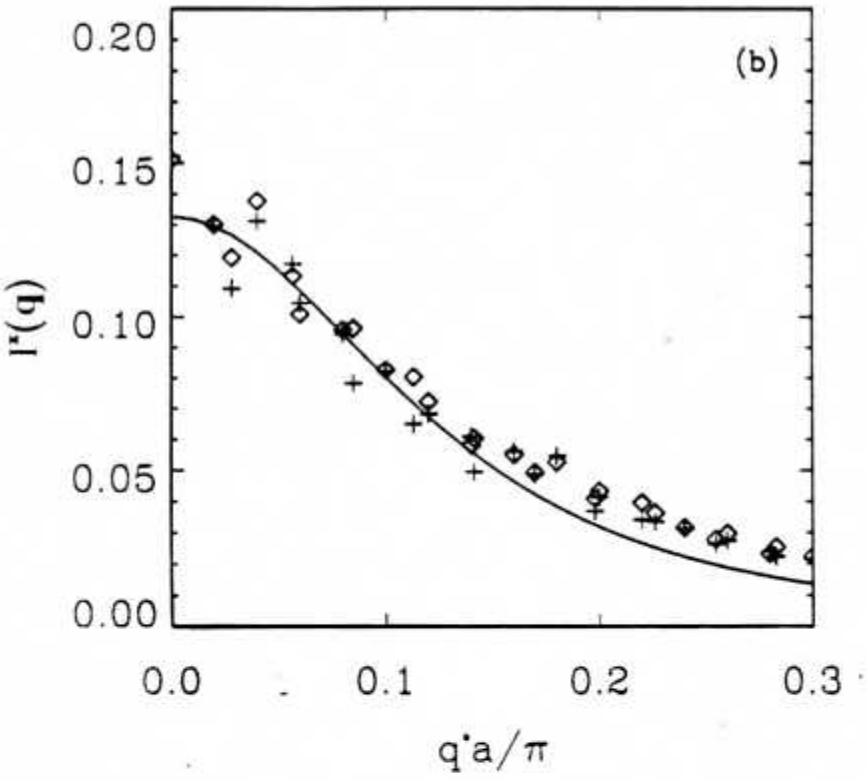

fig 5b

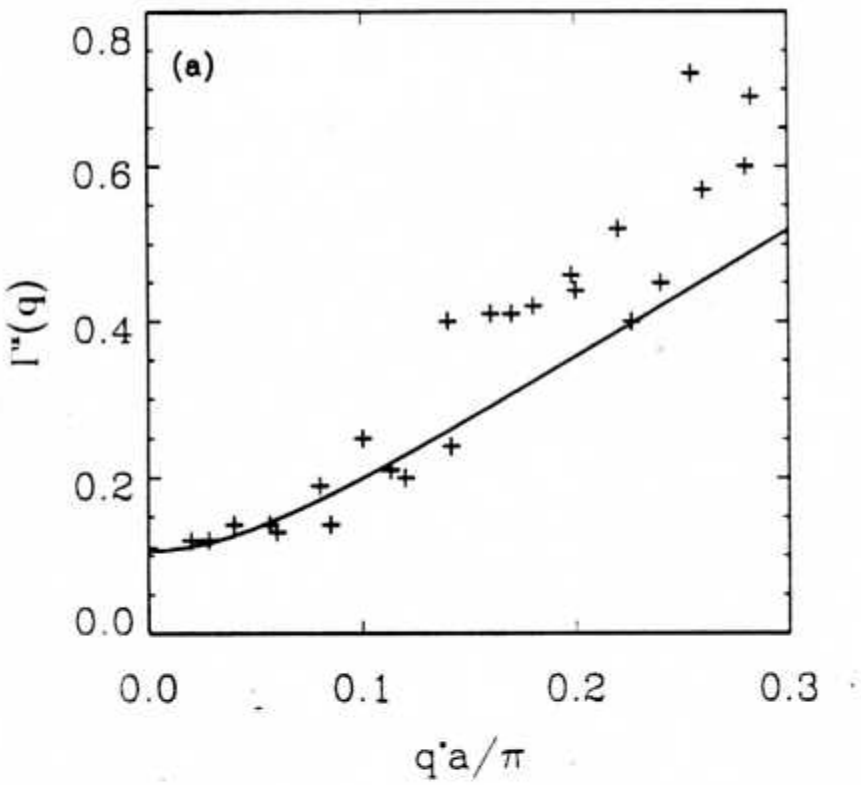

fig 6a

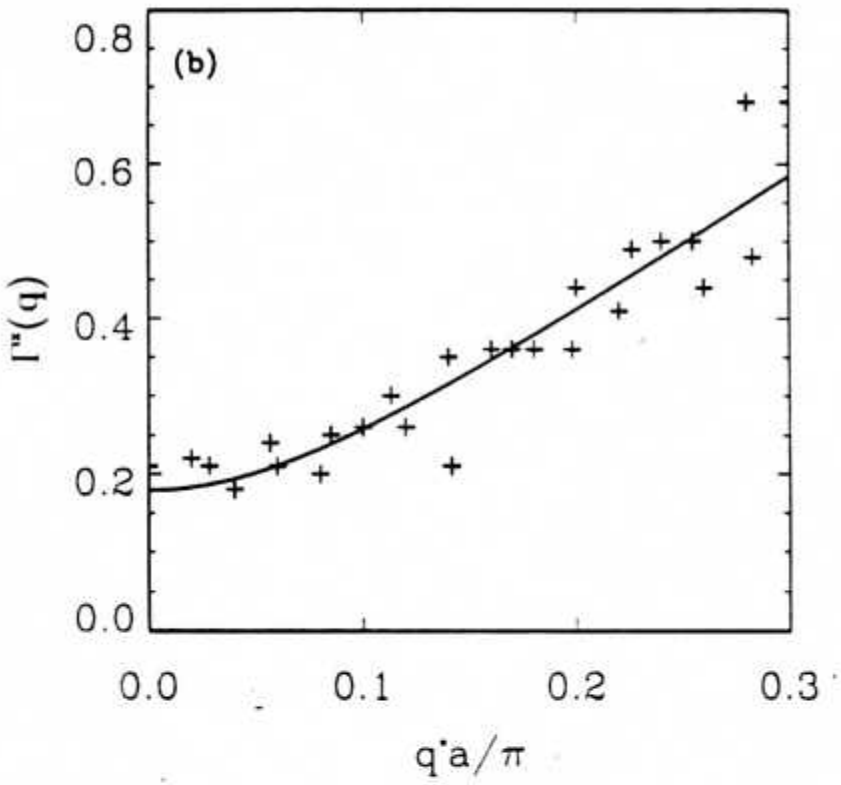

fig 6b

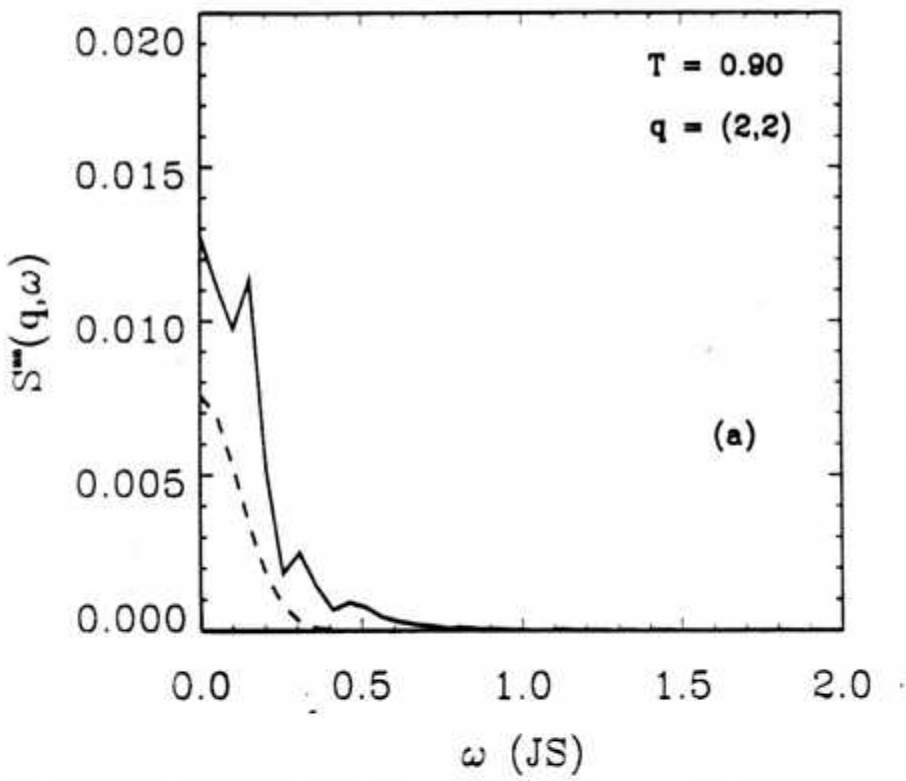
0.020
0.015
0.010
0.005
0.000
$S^{zz}(q,\omega)$
T = 0.90
q = (2,2)
(a)
0.0
0.5
1.0
1.5
2.0
ω (JS)

Fig 7a

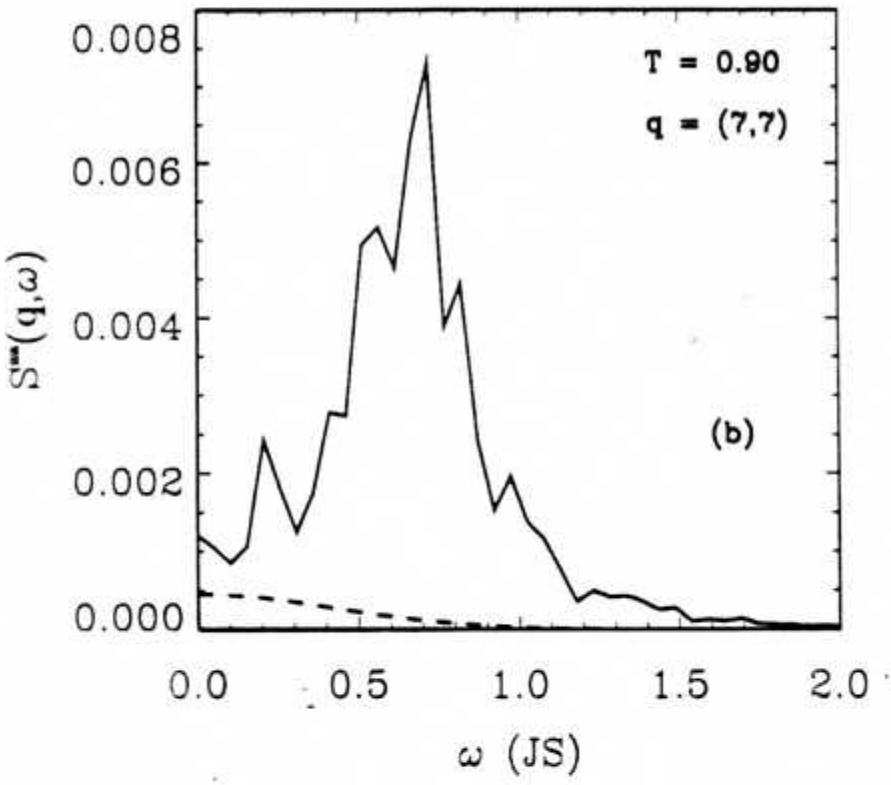
0.008
0.006
0.004
0.002
0.000
$S^{zz}(q,\omega)$
T = 0.90
q = (7,7)
(b)
0.0
0.5
1.0
1.5
2.0
ω (JS)

fig 7b

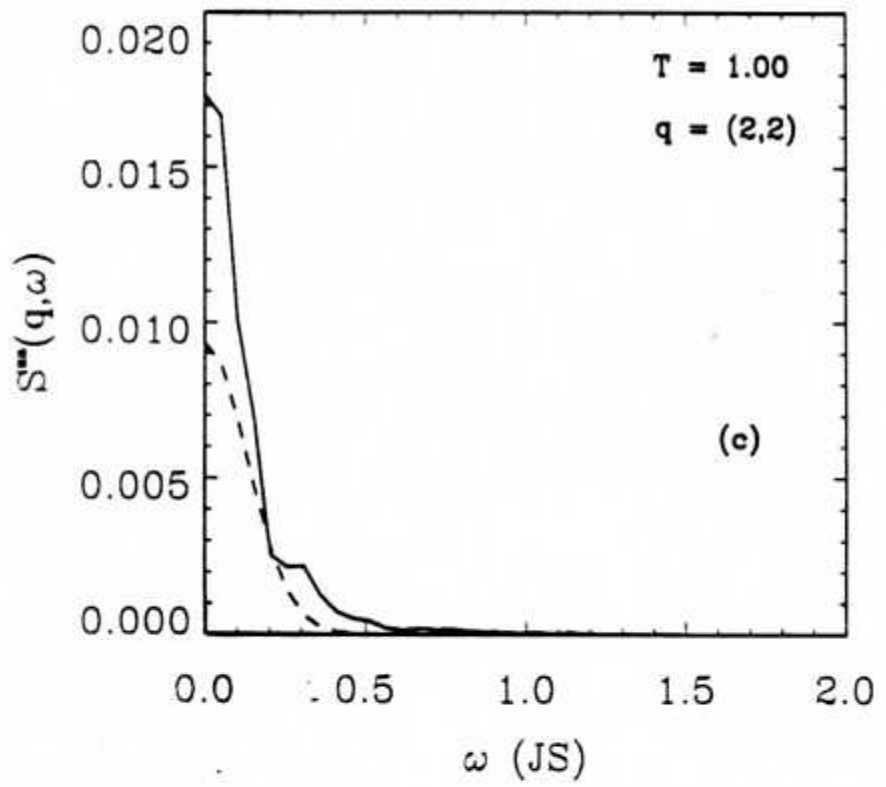
0.020
0.015
0.010
0.005
0.000
$S^{zz}(q,\omega)$
T = 1.00
q = (2,2)
(c)
0.0
0.5
1.0
1.5
2.0
ω (JS)

fig 7c

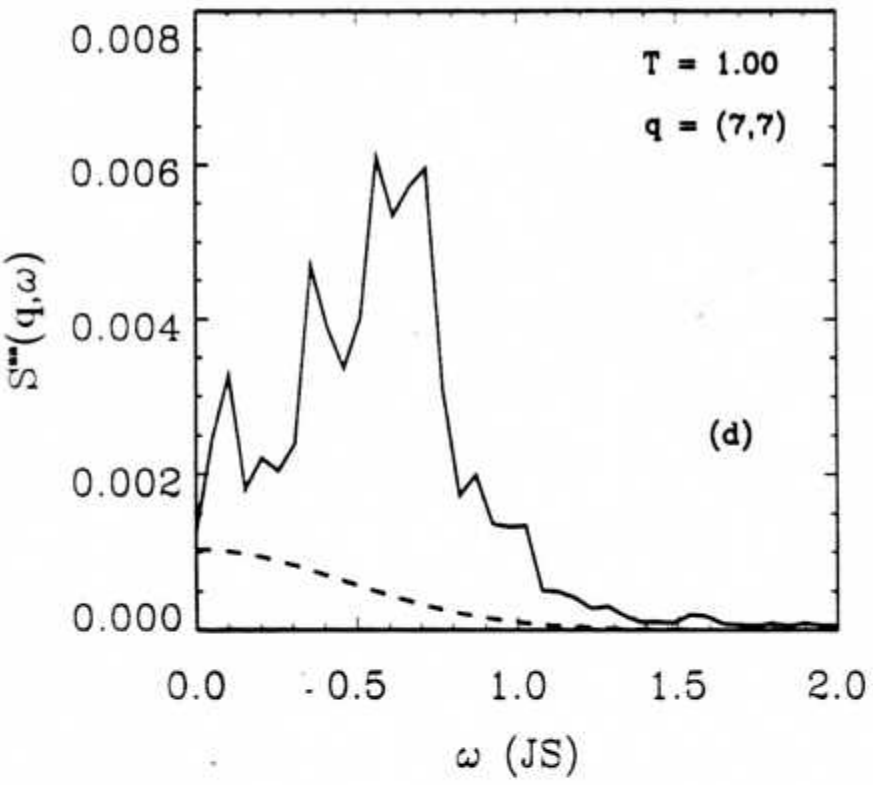

fig 7d.